Supplementary Materials for

Dual-Role Ion Dynamics in Ferroionic $CuInP_2S_6$: Revealing the Transition from Ferroelectric to Ionic Switching Mechanisms

Xingan Jiang[1#], Xiangping Zhang[2#], Zunyi Deng[3#], Jianming Deng[4], Xiaolei Wang[5†], Xueyun Wang[3†] and Weiyou Yang[1†]

[1]Institute of Micro/Nano Materials and Devices, Ningbo University of Technology, Ningbo City,315211, P. R. China

[2]Department of Materials Science and Engineering, Southern University of Science and Technology, Shenzhen, Guangdong 518055, China

[3]School of Aerospace Engineering, Beijing Institute of Technology, Beijing, 100081, China

[4]Guangdong Provincial Key Laboratory of Electronic Functional Materials and Devices, Huizhou University, Huizhou, Guangdong, 516001, China

[5]School of Physics and Optoelectronic Engineering, Beijing University of Technology, Beijing 100124, China.

[†]Corresponding Authors Emails: xiaoleiwang@bjut.edu.cn; xueyun@bit.edu.cn; weiyouyang@tsinghua.org.cn

[#]These authors contribute equally to this work

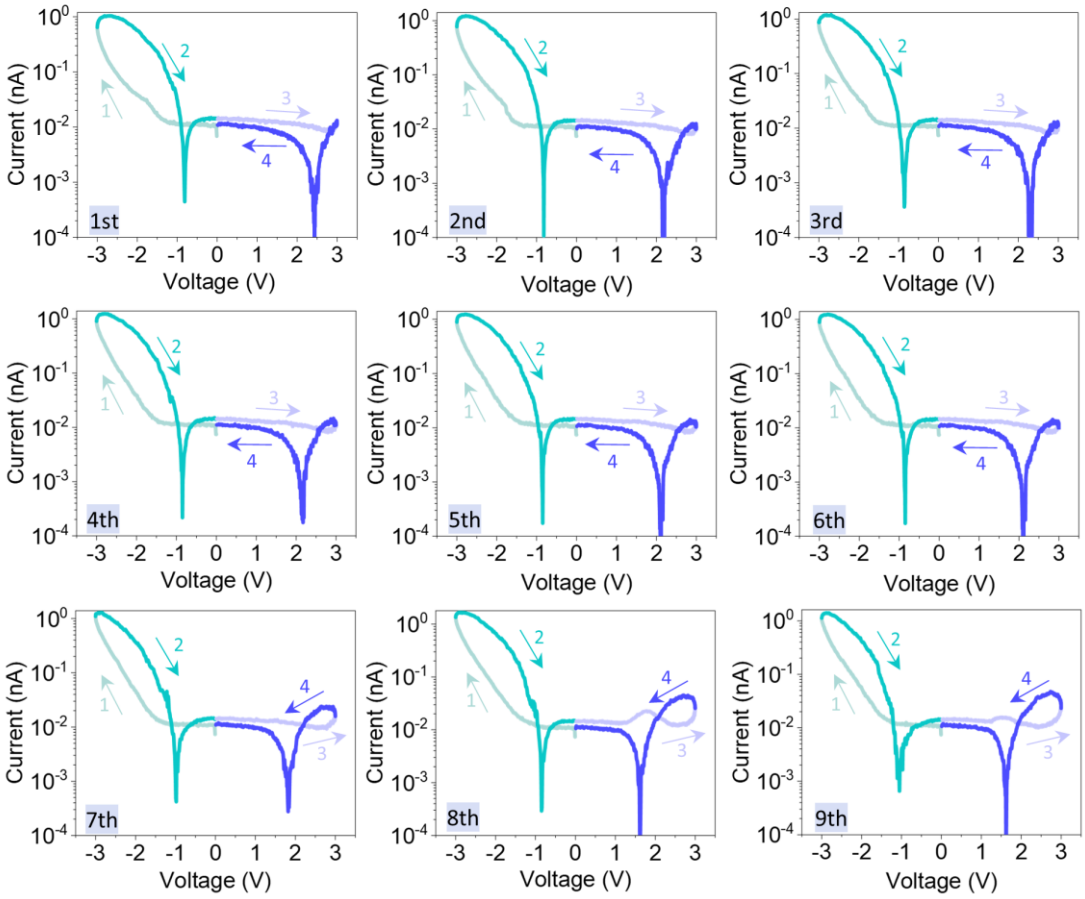

Supplementary Fig. 1. The semilog *I-V* curves using fast scans with a time duration of 1 s for each *I-V* cycle. The raw *I-V* data is adapted from our previous work[1] under a Creative Commons licence CC BY 4.0. With the increased cycles, the current under positive bias gradually increases and forms a visible current hysteresis window, indicating the activated Cu ion migration.

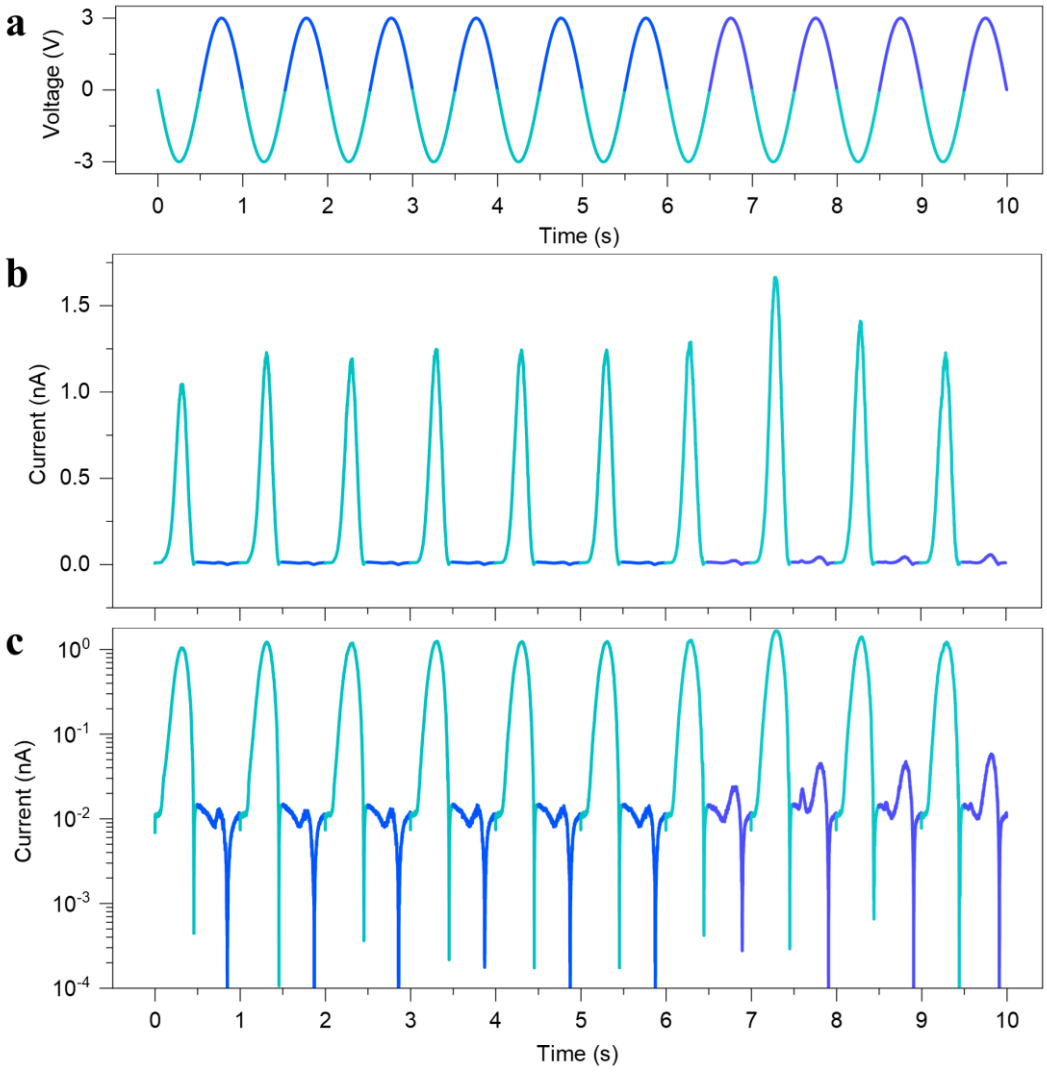

Supplementary Fig. 2. The voltage-time (*V-t*) and current-time (*I-t*) curves for ten sinusoidal voltage sweeping, with a time duration of 1 s for each *I-V* cycle. The raw data is adapted from our previous work[1] under a Creative Commons licence CC BY 4.0. **a** The linear current -time curve. **b** The semilog current-time curve.

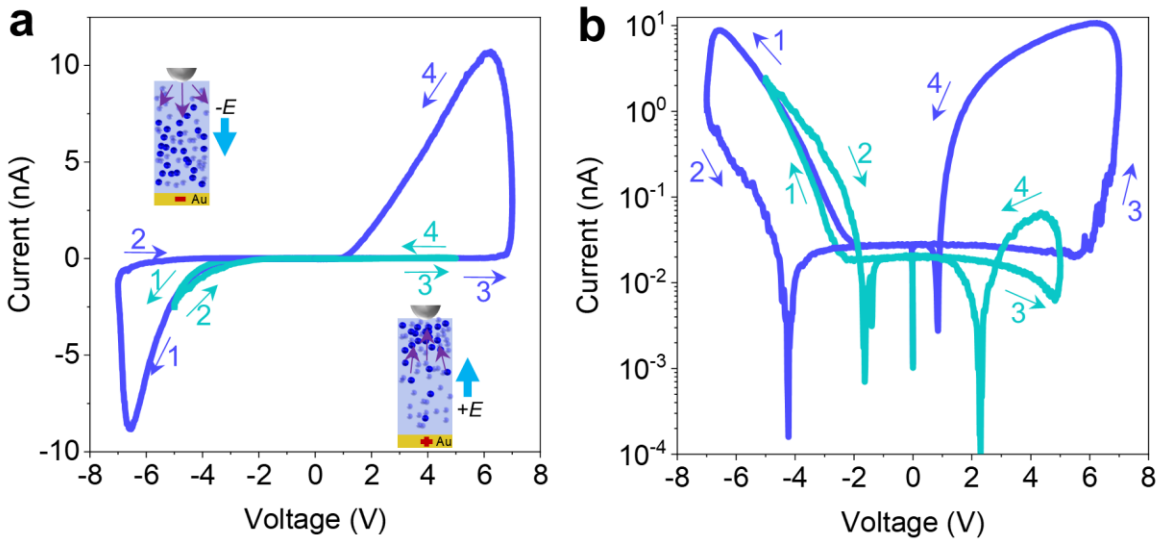

Supplementary Fig. 3. The *I-V* curves conducted at different bias voltage range with time duration of 1 s. a The linear plots of *I-V* curves. The inset shows the accumulation and depletion of Cu ions under positive bias and negative bias, respectively. **b** The semilog plots of *I-V* curves. The number #1-4 and the arrow represents the bias voltage sweeping sequence.

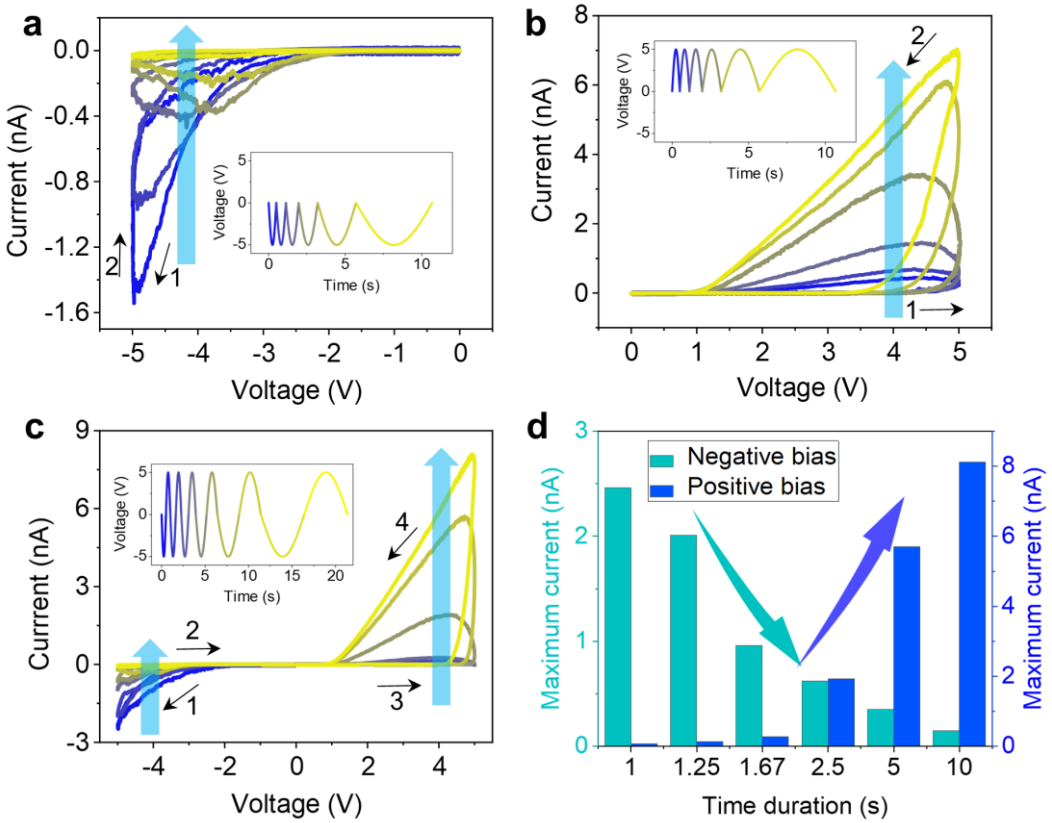

Supplementary Fig. 4. The semi-cycle and full cycle of *I-V* curves conducted using six sinusoidal voltage sweeping with different time duration. a-b The six semi-cycle of *I-V* curves in **(a)** negative and **(b)** positive bias direction with the varied time duration ranging from 0.5 s to 5 s for each semi-cycle, respectively. **c** The six full-cycle of *I-V* curves in two bias direction with the varied time duration ranging from 1 to 10 s for each full-cycle. **d** The maximum current change with the cycles with the varied time duration in two opposite bias direction.

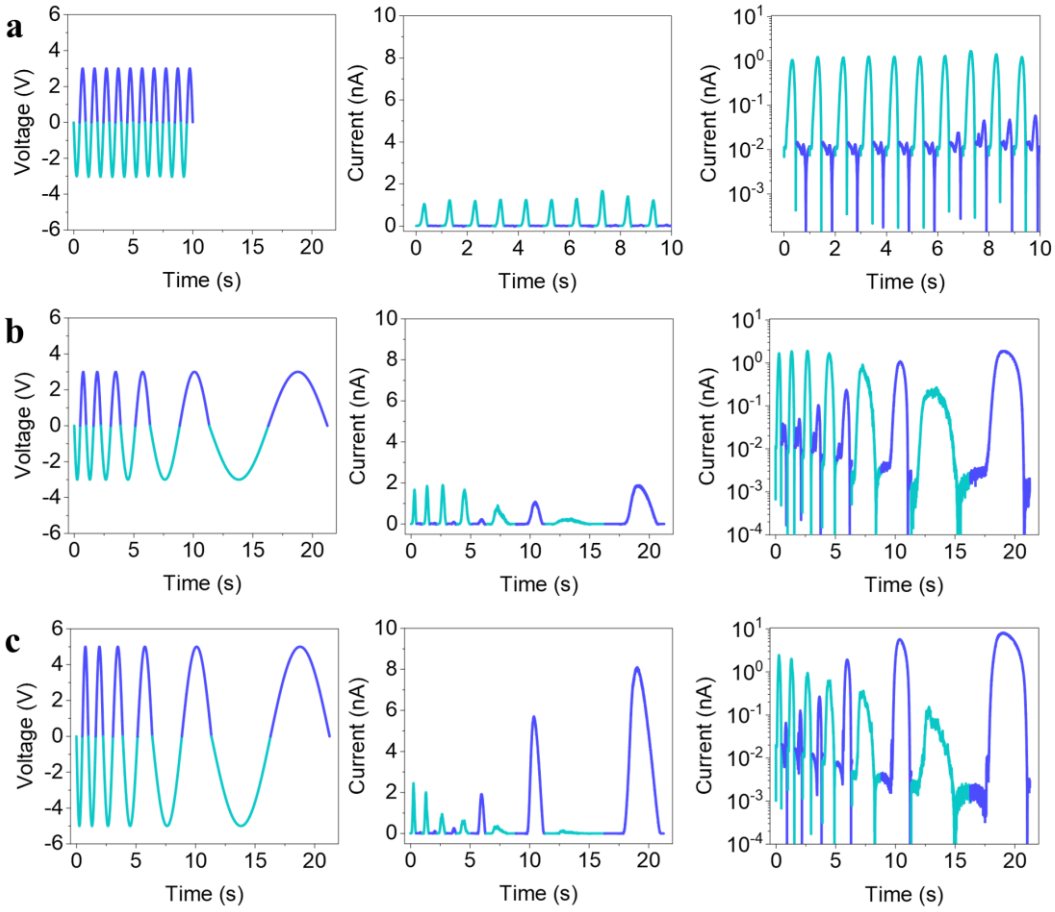

Supplementary Fig. 5. Sinusoidal voltage sweeping cycles and the corresponding current under different bias conditions. The raw data in panel **a** and **b** is adapted from our previous work[1] under a Creative Commons licence CC BY 4.0. **a** Ten sinusoidal voltage sweeping cycles with a maximum voltage V_{max}=3 V and time duration of 1 s for each cycle, and the corresponding current. **b** Six sinusoidal voltage sweeping cycles with V_{max}=3 V and the time duration varying from 1 s to 10 s for each cycle, and the corresponding current. **c** Six sinusoidal voltage sweeping cycles with V_{max}=5 V and time duration varying from 1 s to 10 s for each cycle, and the corresponding current.

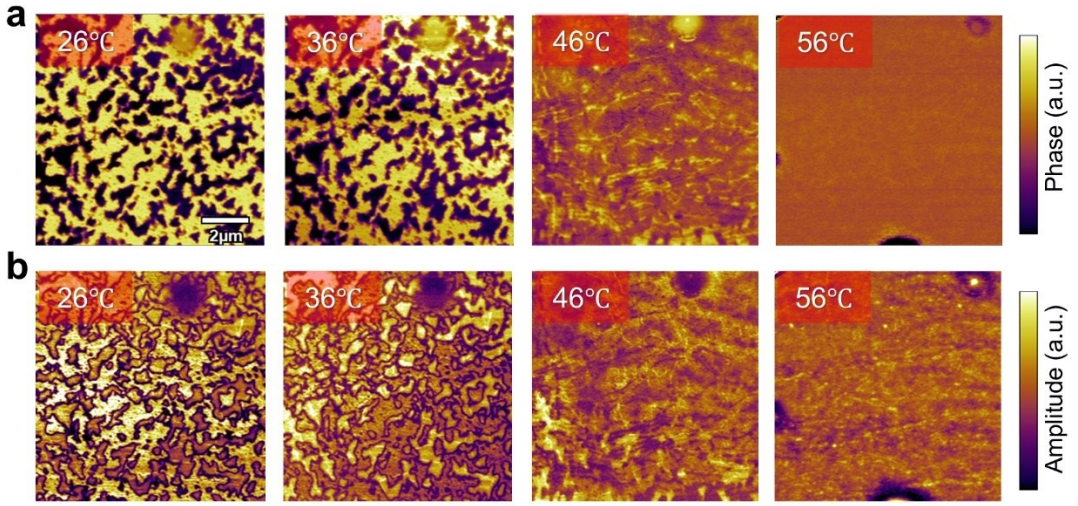

Supplementary Fig. 6. The in-situ variable temperature PFM images. a-b The phase and amplitude at four set of temperatures (26 ℃, 36 ℃, 46 ℃, and 56 ℃), respectively. When the temperature exceeds 46 ℃, ferroelectricity begins to rapidly disappear.

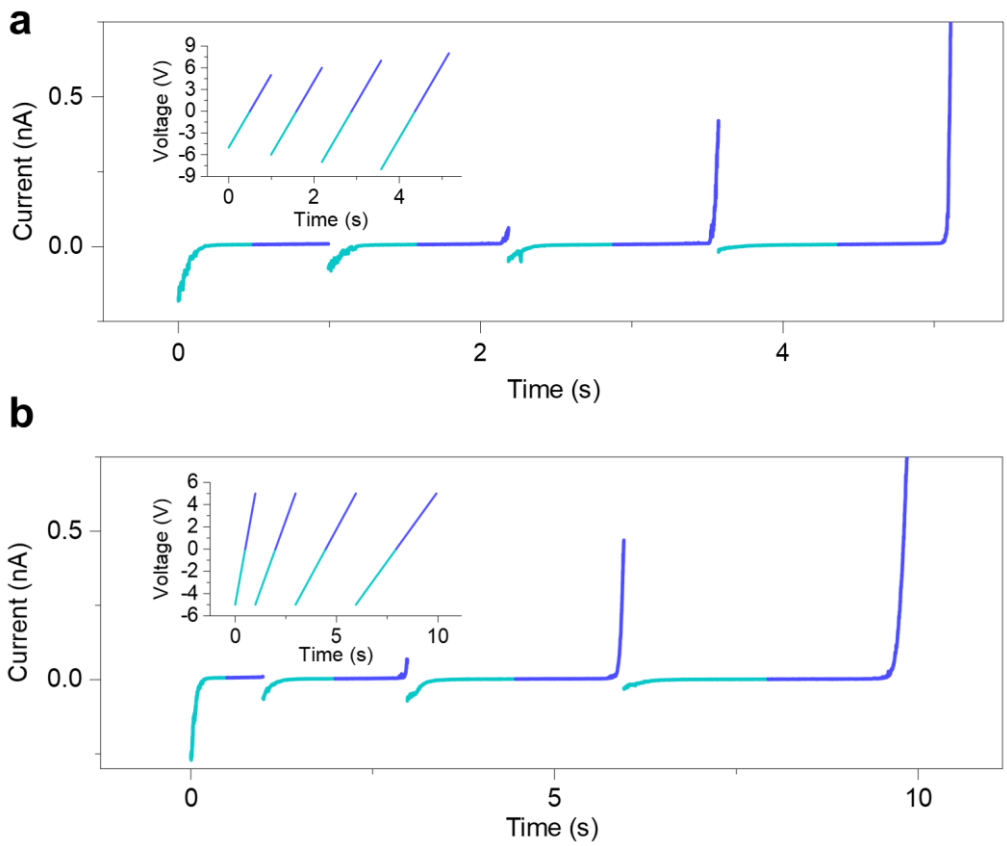

Supplementary Fig. 7. Reversed current rectification with increased bias voltage magnitude and longer time duration. a The varied bias voltage magnitude with V_{max} ranging from 5 V to 8 V and time duration is 1 s for each cycle, and the corresponding current. **b** The varied time duration ranging from 1 s to 4 s for each *I-V* curve with V_{max}=5 V, and the corresponding current.

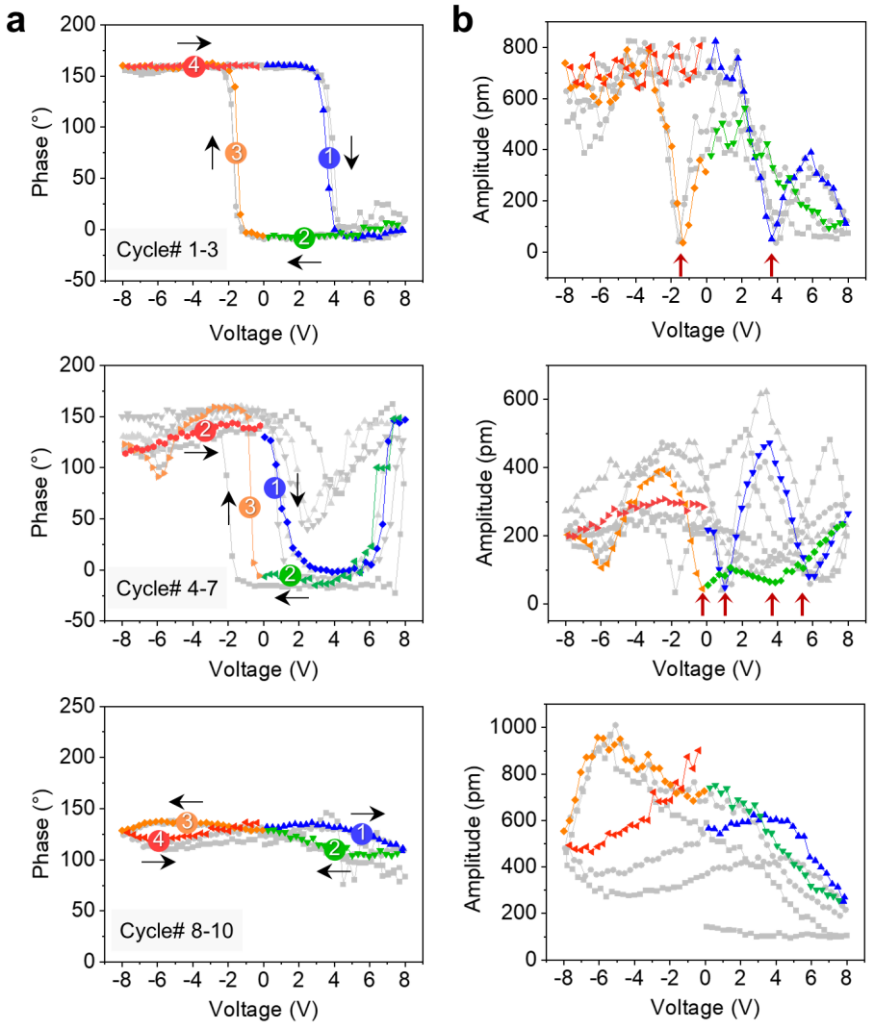

Supplementary Fig. 8. Ten SS-PFM performed at a specific location with time duration of 1 s for each *I-V* cycle. a, b The phase and amplitude at different test cycles, respectively. The numbers#1-4 and black arrows represent the bias scanning sequence and direction, respectively.

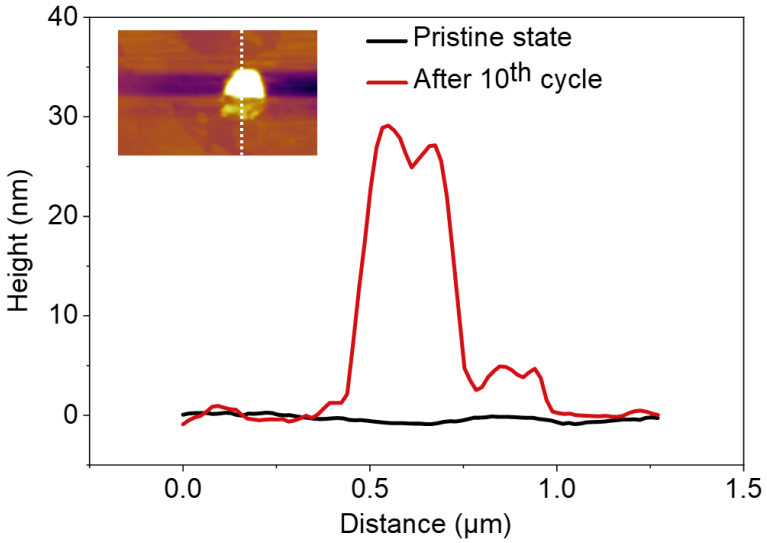

Supplementary Fig. 9. The topography height changes before and after ten SS-PFM measurements performed at a specific location. The long-range migration across the vdW gap significantly disrupts the ferroelectric order, which is further confirmed by the formation of topographic bulges up to 30 nm after 10 cycles.

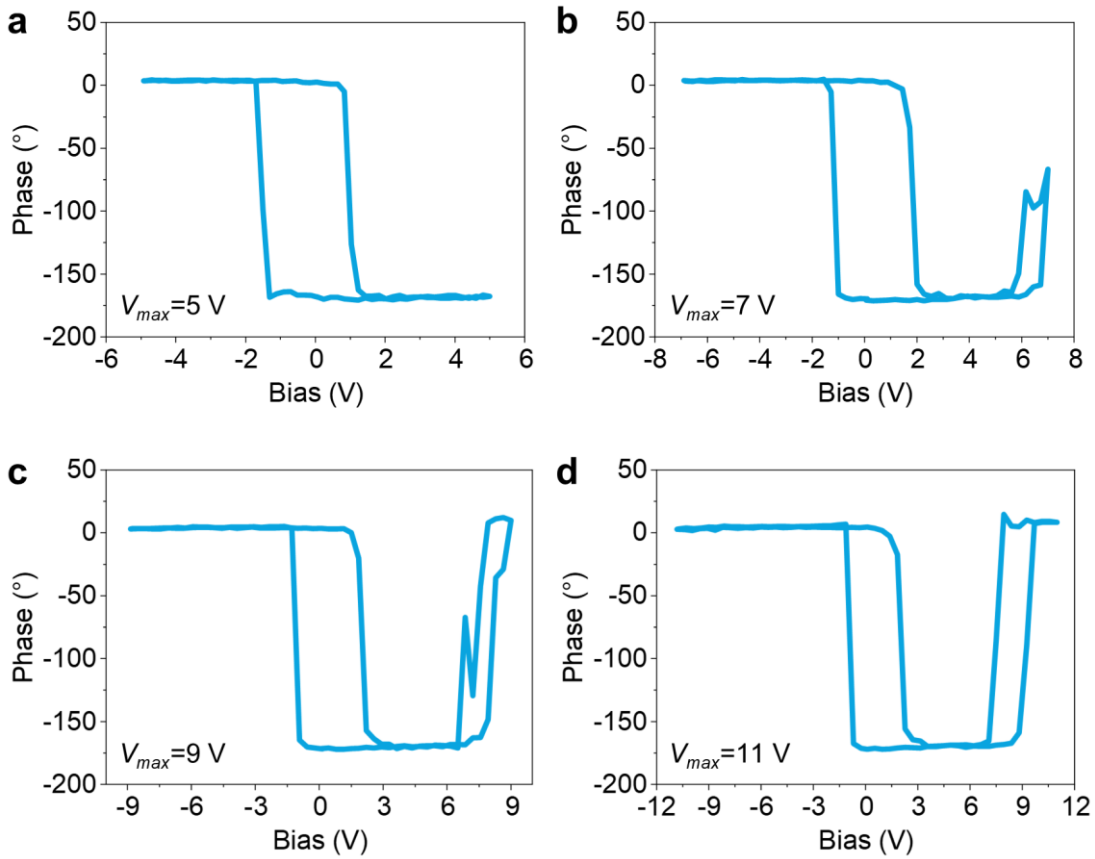

Supplementary Fig. 10. The abnormal switching behaviors modulated by tuning the bias magnitude. a-d The SS-PFM loop measured at different V_{max}, corresponding to V_{max}=5 V, V_{max}=7 V, V_{max}=9 V, and V_{max}=11 V, respectively. The time duration for each loop is 1 s.

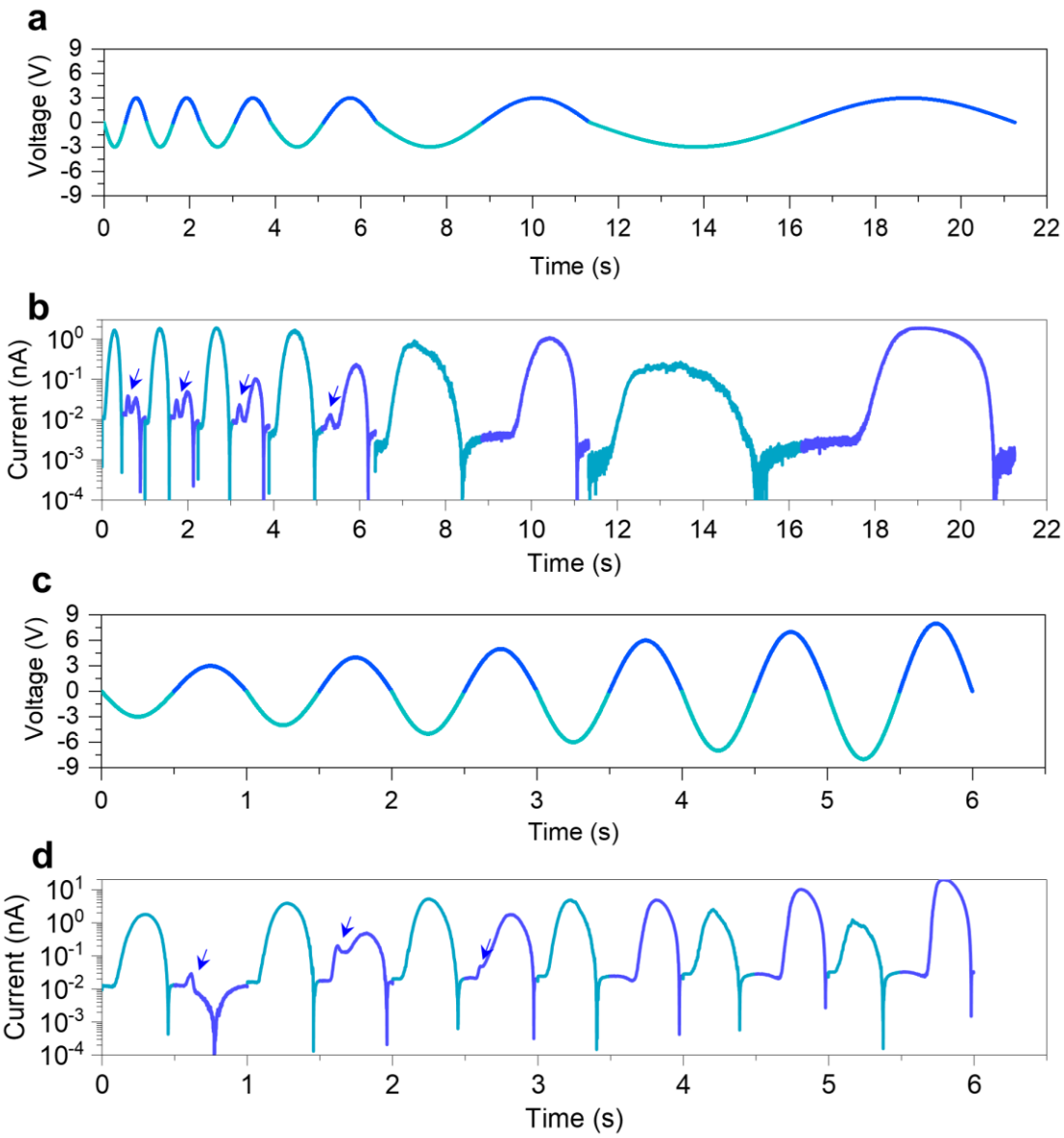

Supplementary Fig. 11. Six sinusoidal voltage sweeping cycles and the corresponding current versus the time duration for six cycles under different bias condition. The raw data is adapted from our previous work[1] under a Creative Commons licence CC BY 4.0. **a-b** Six sinusoidal voltage sweeping cycles with the varied time duration ranging from 1 s to 10 s and the corresponding current. **c-d** Six sinusoidal voltage sweeping cycles with a time duration of 1 s and the varied bias voltage magnitude ranging from 3 V to 8 V and the corresponding current.

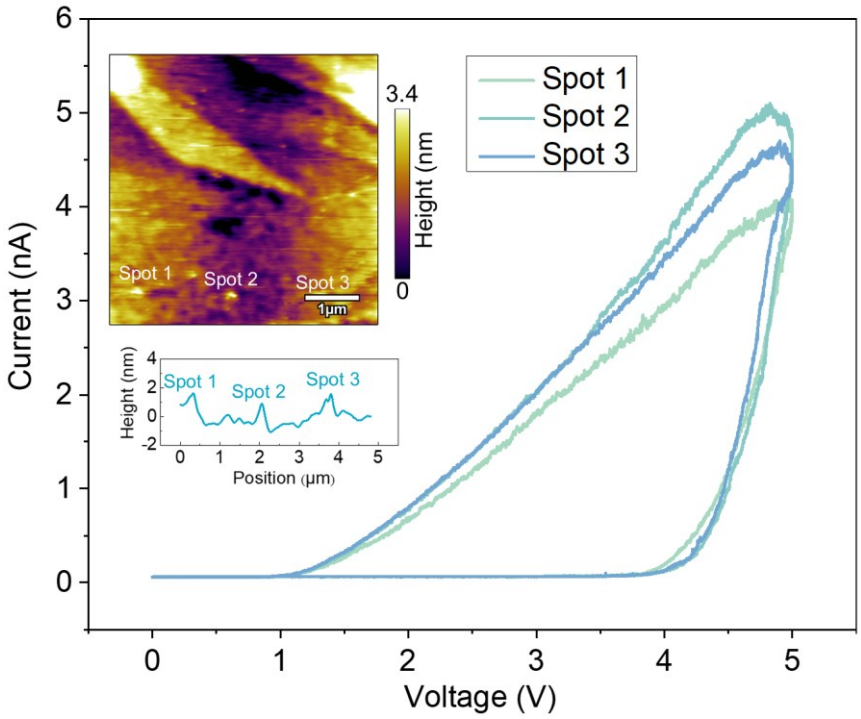

Supplementary Fig. 12. The semi-cycle of I-V curves measured by the sequence of (0 V→+5 V→0 V) at three different positions and the topographic changes. A slightly topographic bump (~2 nm) appears due to the long-range migration and redistribution of Cu^{+} ions.

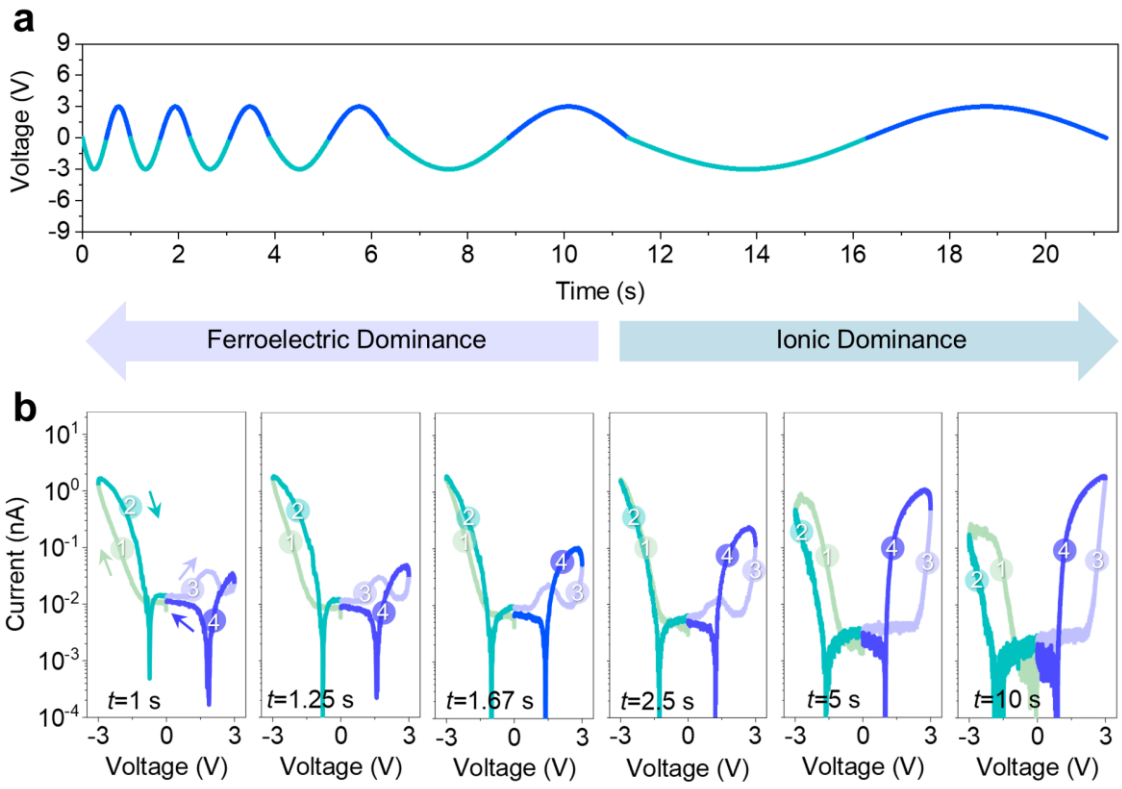

Supplementary Fig. 13. Six sinusoidal voltage sweeping cycles with the varied time duration for each cycle and the corresponding six full-cycle of semilog *I-V* curves. The raw data is adapted from our previous work[1] under a Creative Commons licence CC BY 4.0. **a** Six sinusoidal voltage sweeping cycles and the corresponding time duration varies from 1 s to 10 s for each cycle. **b** The corresponding six full-cycle of semilog *I-V* curves as the time duration varies from 1 s to 10 s.

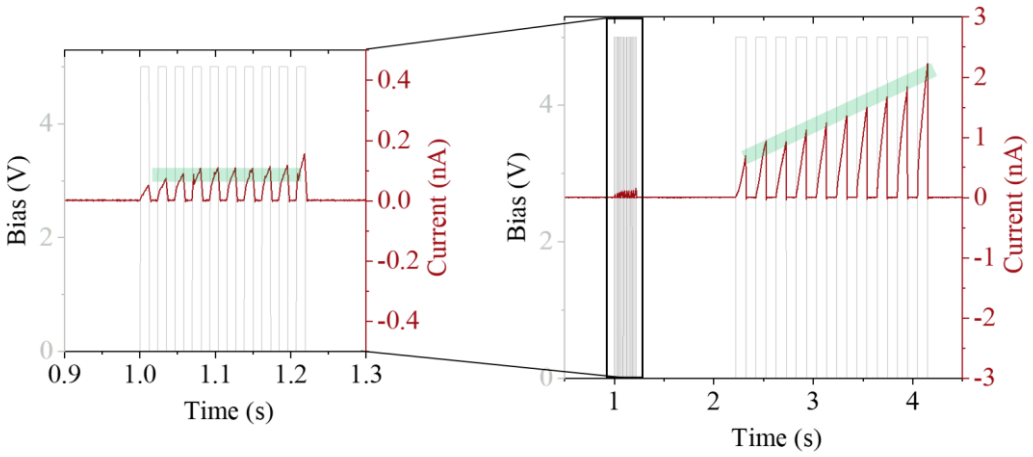

Supplementary Fig. 14. The current in response to two different pulse conditions. The current was measured in response to ten consecutive 5 V pulse cycles with pulse widths of 0.01 s and 0.1 s, respectively.

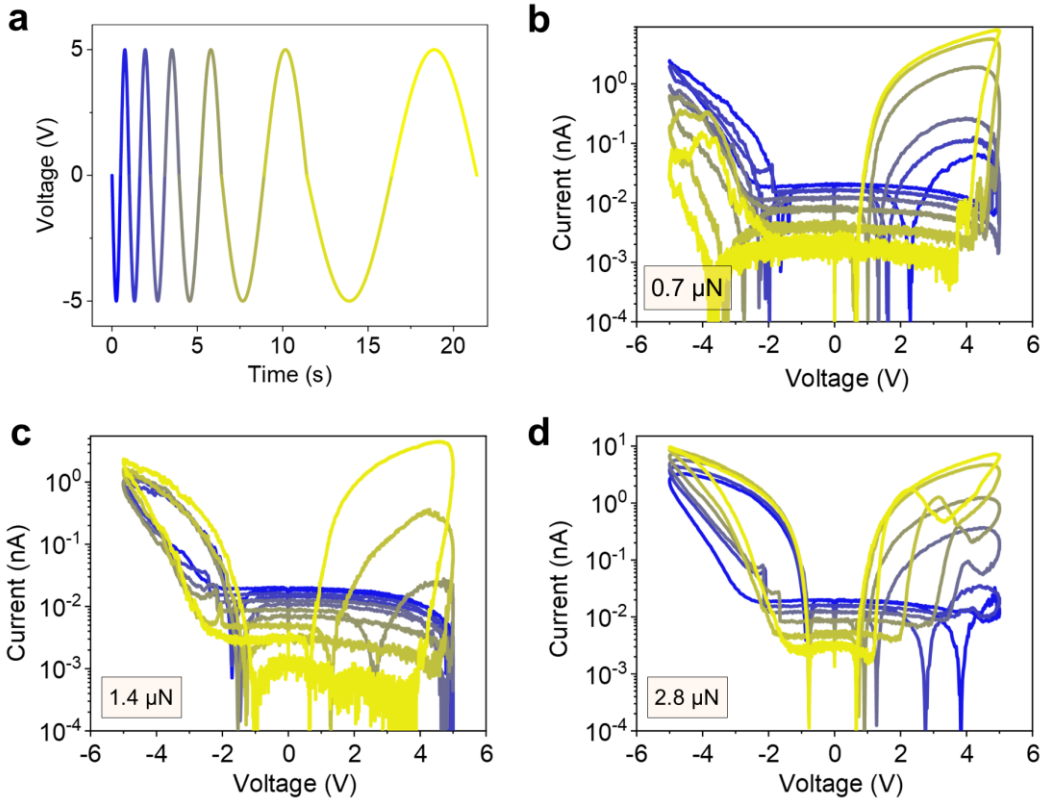

Supplementary Fig. 15. Six sinusoidal voltage sweeping cycles with the varied time duration for each cycle and the corresponding six full-cycle of semilog *I-V* curves at different tip force. a Six sinusoidal voltage sweeping cycles and the corresponding time duration varies from 1 s to 10 s for each cycle. **b-d** The six full-cycle of semilog *I-V* curves under 0.7 μN, 1.4 μN and 2.8 μN, respectively.

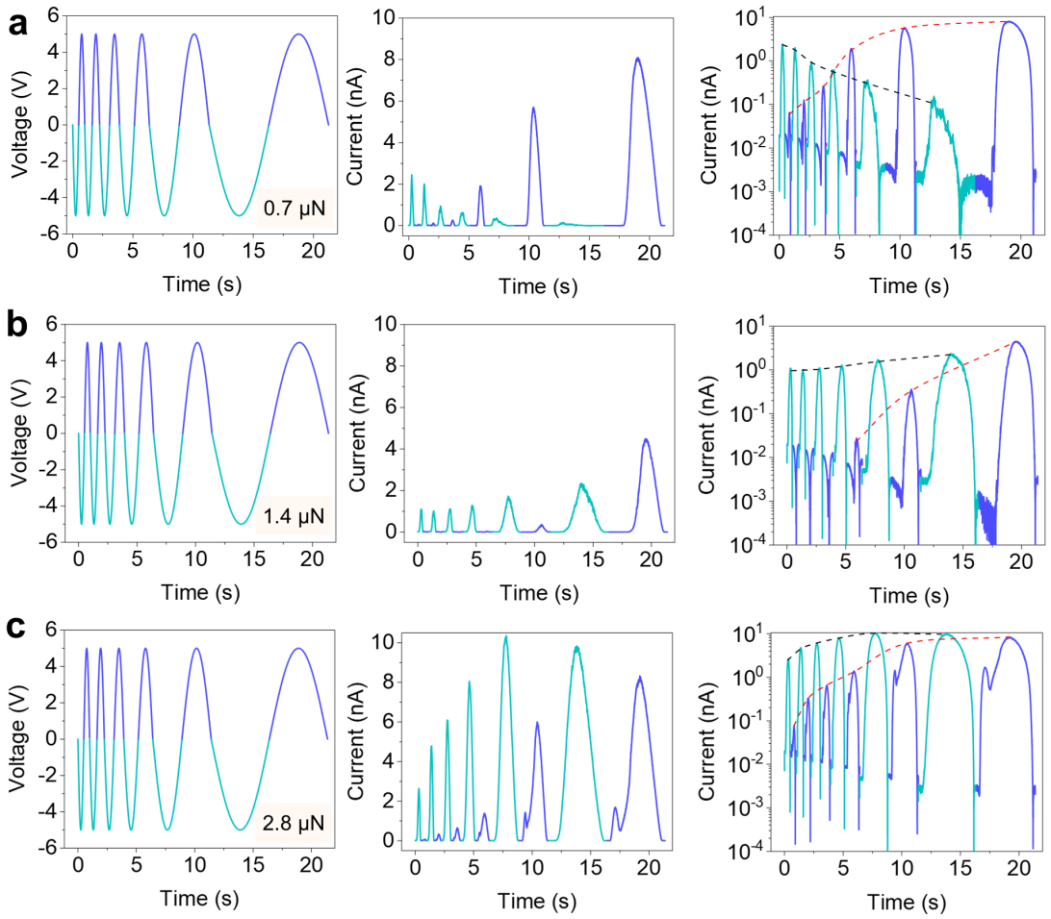

Supplementary Fig. 16. Six sinusoidal voltage sweeping cycles with the varied time duration for each cycle under three different tip forces and the corresponding current. a-c Six voltage sweeping cycles with the varied time duration from 1 s to 10 s and the corresponding current under **(a)** 0.7 μN, **(b)** 1.4 μN, and **(c)** 2.8 μN, respectively.

Supplementary Table 1. Lattice parameters (*a*, *b*, *c* and β) and lattice volume *V* of bulk CIPS calculated with various exchange-correlation functionals. Experimental and other theoretical lattice parameters at 295 K are also listed for comparison.

Methods	*a* (Å)	*b* (Å)	*c* (Å)	β (°)	*V* (Å^3)
PBE+DFT-D2	6.091	10.546	13.788	107.27	845.77
PBE+DFT-D3(0)	6.108	10.580	13.835	107.21	854.05
PBE+DFT-D3(BJ)	6.070	10.512	13.543	107.34	824.35
PBEsol+DFT-D2	5.979	10.341	13.197	107.69	777.36
PBEsol+DFT-D3(0)	6.015	10.415	13.386	107.41	800.22
PBEsol+DFT-D3(BJ)	5.971	10.352	12.974	107.10	766.55
PBE+DFT-D3(BJ)[2]	6.068	10.510	13.510	107.34	822.4
Exp. (295 K)[3]	6.0956	10.5645	13.6230	107.101	838.5

References

1. Jiang, X. *et al*. Manipulation of current rectification in van der Waals ferroionic $CuInP_2S_6$. *Nat. Commun.* **13**, 574 (2022).
2. Zhang, X. *et al*. Origin of versatile polarization state in $CuInP_2S_6$. *Phy. Rev. B* **108**, L161406 (2023).
3. Maisonneuve, V. *et al*. Ferrielectric ordering in lamellar $CuInP_2S_6$. *Phy. Rev. B* **56**, 10860 (1997).